Molecular Vision 2006; 12:774-90 <http://www.molvis.org/molvis/v12/a87/>
Received 12 April 2005 | Accepted 22 June 2006 | Published 12 July 2006

Genome-wide expression profile of human trabecular meshwork cultured cells, nonglaucomatous and primary open angle glaucoma tissue

Paloma B. Liton, Coralia Luna, Pratap Challa, David L. Epstein, Pedro Gonzalez

Department of Ophthalmology, Duke University, Durham, NC

Purpose: To contrast genome-wide gene expression profiles of cultured human trabecular meshwork (HTM) cells to that of control and primary open angle glaucoma (POAG) HTM tissues.
Methods: Cultured HTM cells, HTM tissue dissected from control donors, and HTM tissue from POAG donors receiving medication for glaucoma were fixed in RNA later™. Total RNA extracted from these samples was linearly amplified with the Ovation Biotin RNA Amplification and Labeling System and individually hybridized to Affymetrix Human Genome U133 Plus 2.0 high density microarrays. Data analysis was performed using GeneSpring Software 7.0. Selected genes showing significant differential expression were validated by quantitative real-time PCR in nonamplified RNA.
Results: Cultured HTM cells retained the expression of some genes characteristic of HTM tissue, including chitinase 3-like 1 and matrix Gla protein, but demonstrated downregulation of physiologically important genes such as myocilin. POAG HTM tissue showed relatively small changes compared to that of control donors. These changes included the statistically significant upregulation of several genes associated with inflammation and acute-phase response, including selectin-E (*ELAM-I*), as well as the downregulation of the antioxidants paraoxonase 3 and ceruloplasmin.
Conclusions: Downregulation in cultured HTM cells of genes potentially relevant for outflow pathway function highlights the importance of developing new conditions for the culture of TM cells capable of preserving the characteristics of TM cells in vivo. Comparative analysis between control and POAG tissues suggests that the upregulation of inflammation-associated genes might be involved in the progression of glaucoma.

The conventional outflow pathway, consisting of the trabecular meshwork (TM) and Schlemm's canal (SC), is a highly specialized tissue located at the angle formed by the cornea and iris. This tissue is involved in intraocular pressure (IOP) homeostasis by modulating the outflow of aqueous humor (AH) from the anterior chamber to the venous system. Increased IOP resulting from abnormally high outflow resistance is commonly associated with primary open angle glaucoma (POAG) [1-3].

In addition to modulating AH outflow resistance, the conventional outflow pathway is believed to be involved in detoxification of the AH, phagocytosis of cellular debris, and the maintenance of immune privilege in the eye. To accomplish all these functions, the conventional outflow pathway is organized, despite its small size (100-150 µg, containing approximately 200,000-300,000 cells), as a complex structure composed of morphologically and functionally different cell types: the Schwalbe's line (SL) cells, proposed to be the progenitor cells of the TM [4,5]; TM cells, involved in phagocytosis and tissue remodeling; and juxtacanalicular tissue (JCT) cells that, together with the cells of the inner wall of SC, contain the locus for outflow resistance [6,7]. The physiological mechanisms by which the TM/SC outflow pathway regulates the outflow of AH, as well as the cause for the increase in resistance leading to elevated IOP in POAG, remain unknown.

Over the last decade, gene expression profiling has emerged as one of the most powerful approaches for dissecting the regulatory mechanisms and transcriptional networks that underlie biological processes. Although several laboratories, including ours, have extensively worked to define the gene expression profile of the outflow pathway, there is still incomplete information available, mainly due to the small amount of RNA that can be isolated from each sample. To date, two different cDNA libraries from human TM (HTM) tissue have been reported. Using single-pass sequencing, Gonzalez et al. [8] described the 833 genes more highly expressed in a PCR-amplified cDNA library constructed from the TM of a perfused human anterior segment of a single individual. Tomarev et al. [9] identified the 3,459 genes more highly expressed in a cDNA library constructed from a pool of native TM from 28 donors. Although these two libraries have provided important information regarding the genes that are more highly expressed in the TM, we still lack critical information about genes with lower expression that still might be essential for tissue function.

To generate a genome-wide gene expression profile of the TM and identify genes associated with the maintenance of tissue physiology, we performed microarray analysis in both native TM tissue and cultured HTM cells. We used the new Affymetrix Human Genome U133 Plus 2.0 Array in conjunc-

Correspondence to: Pedro Gonzalez, Duke University Eye Center, Erwin Road, Box 3802, Durham, NC, 27710; Phone: (919) 681-5995; FAX: (919) 684-8983; email: pedro.gonzalez@duke.edu

tion with a novel linear mRNA amplification method, RiboSPIA, recently introduced by NuGEN technologies. In addition, we have analyzed, for the first time, the gene expression profile of TM tissue from POAG donors.

METHODS

Human tissue procurement: Human cadaver eyes from donors were obtained from the North Carolina Eye Bank (NCEB). The anterior segments of the five pairs of eyes used for the gene expression profile of TM tissue included three control pairs of eyes without known history of glaucoma and two pairs of eyes from donors with documented history of POAG and glaucoma medication (Table 1). All eyes were enucleated less than 6 h postmortem and immediately fixed in RNA later™ (Ambion Inc., Austin, TX) to preserve RNA integrity. The anterior segments of the three pairs of eyes used for gene expression profile of cultured TM cells were obtained less than 24 h postmortem and immediately immersed in Optisol. Ocular histories were carefully reviewed by a certified ophthalmologist. Tissues from eye donors were manipulated at all times in accordance to the Tenets of the Declaration of Helsinki.

Human trabeculr meshwork primary cultures: Primary cultures of HTM were prepared from cadaver eyes following previously described guidelines [10] and maintained at 37 °C in a humidified atmosphere of 5% CO_2 in low glucose Dulbecco's Modified Eagle Medium (DMEM) with L-glutamine and 110 mg/l sodium pyruvate, supplemented with 10% fetal bovine serum (FBS), 100 μM nonessential amino acids, 100 units/ml penicillin, 100 μg/ml streptomycin sulfate and 0.25 μg/ml amphotericin B. All reagents were obtained from Invitrogen Corporation (Carlsbad, CA).

RNA extraction and quality analysis: Total RNA, from dissected TM tissues and RNA later-fixed cultured HTM cells at passage three, was isolated using the RNeasy kit (Qiagen Inc., Valencia, CA) following the manufacturer's protocol. After DNase treatment, RNA yields were determined using the RiboGreen® fluorescent dye (Molecular Probes Inc., Eugene, OR). RNA quality was confirmed by assessing the ratio of ribosomal bands 28S and 18S, using the Agilent 2100 Bioanalyzer.

RNA amplification and cDNA biotin labeling: RNA samples were amplified using the Ovation™ Biotin RNA amplification and Labeling System (NuGEN Technologies Inc., San Carlos, CA) according to the manufacturer's instructions. Briefly, total RNA (20 ng) was reverse transcribed into cDNA using a reverse transcriptase and a DNA/RNA chimeric primer. This strand is copied by a DNA polymerase with reverse transcriptase activity to give double-stranded cDNA with

Table 1.

Sample type	Sample name	Age/ Sex/ Race	Cause of death	Other ocular disease	IOP	Treatment
HTM Cells	HTM-A	45/F/C	Multisystem organ failure			
	HTM-B	25/F/C	Pneumonia			
	HTM-C	58/M/C	Cancer			
Control	C-A	70/F/C	IC bleed			
	C-B	85/F/C	IC bleed			
	C-C	78/M/AA	Abdominal aortic aneurism			
POAG	P-A	59/M/C	Renal failure	Cataracts	17-28	Xalatan (Latanoprost; 17 months)
	P-B	77/F/AA	Renal failure	Cataracts, Diabetes	15-25	Xalatan, Cosopt (Dorzolamide hydrochloride, Timolol maleate; >12 months)

Summary of the information for the donors used in this study, including history of glaucoma treatments.

an RNA-DNA heteroduplex at one end. This double-stranded cDNA is amplified using the novel isothermal linear amplification method Ribo-SPIA™ (NuGEN Technologies Inc.). The cDNA amplification products were fragmented and labeled to generate biotinylated cDNA targets.

Oligonucleotide microarray analysis: Biotinylated cDNA targets were hybridized on Affymetrix Human Genome U133 Plus 2.0 high density microarrays following the manufacturer's instructions. A total of eight cDNA target preparations were performed, and each preparation was analyzed using one microarray. Data analysis was performed using GeneSpring Software 7.0 (Silicon Genetics, Redwood City, CA). Raw data from eight hybridizations were normalized to the fiftieth percentile per chip and to median per gene. Normalized mean values for the three individual experimental groups (cultured TM cells, control, and POAG) were generated for the experimental interpretation. Genes with a differential expression of two fold were selected and then filtered on flags to retain the genes that were presented in all samples of at least one of the experimental groups. Statistical analyses were performed by using the cross-gene-error model in combination with a one-way ANOVA ($p<0.05$). Since some genes were represented in the arrays in more than one spot, we verified a consistent differential expression in all the spots to eliminate false positives.

Quantitative real-time PCR: First strand cDNA was synthesized from a pool of total RNA (0.5 μg, equal amounts of each individual sample) by reverse transcription using oligodT

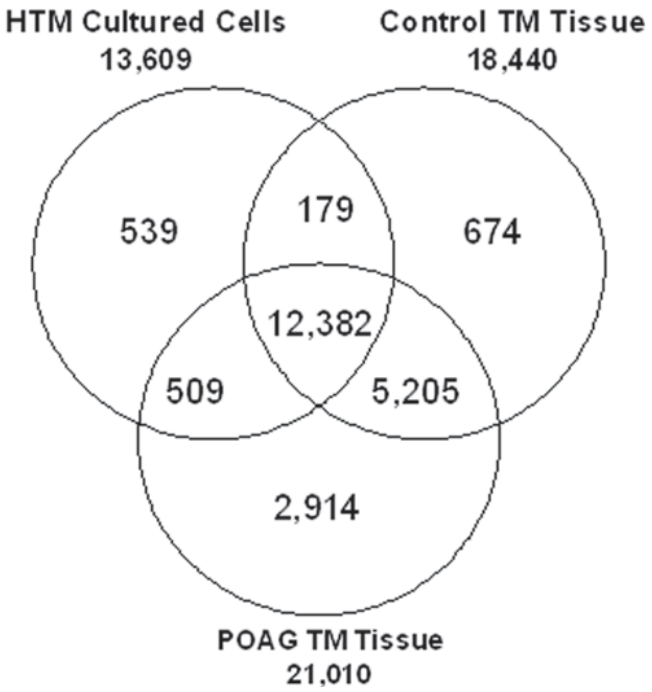

Figure 1. Venn diagrams showing the transcriptional profile distribution between cultured human trabecular meshwork (HTM) cells, control trabecular meshwork (TM) tissue, and POAG TM tissue.

Table 2. Sequences of the primers used for real-time PCR analysis.

Gene	Primer sequences	Gene	Primer sequences
ADORA3	F: 5'-ATCGCTGTGGACCGATACTT-3'	MGP	F: 5'-CCAAGAGAGGATCCGAGAACG-3'
	R: 5'-GGCCAGCCATATTCTTCTGT-3'		R: 5'-ATCCATAAACCATGGCGTAGC-3'
APOD	F: 5'-AACCTTTGAGAATGGACGCT-3'	MKK6	F: 5'-CACAGAGACGTCAAGCCTTC-3'
	R: 5'-GGCTTCACCTTCGATTTGAT-3'		R: 5'-CAGAGTCCACCAAGTAGCCA-3'
AQP1	F: 5'-CAATGACCTGGCTGATGGT-3'	MMP10	F: 5'-TGCATCAGGCACCAATTTAT-3'
	R: 5'-GGTAGTAGCCAGCACGCATA-3'		R: 5'-TGTTGGCTGAGTGAAAGAGC-3'
BCL2A1	F: 5'-TCAACAGCTTCAAGGTGAGC-3'	MMP3	F: 5'-GCCAGGGATTAATGGAGATG-3'
	R: 5'-ACGCACTGCAGATAGTCCTG-3'		R: 5'-ATTTCATGAGCAGCAACGAG-3'
CDH10	F: 5'-CCTGAAACAGGTATCATCAGGA-3'	MYOC	F: 5'-CTGGCTATCTCAGGAGTGGAG-3'
	R: 5'-AGCGTGATGTTCACAGTGGT-3'		R: 5'-CGCATCCACACACCATACTT-3'
CALB1	F: 5'-GCTGACGGAAGTGGTTACCT-3'	PODXL	F: 5'-CCAGAATGCAACCCAGACTA-3'
	R: 5'-TCTTTGCCCATACTGATCCA-3'		R: 5'-CTGGGCTGTATCTGTAGCCA-3'
CDT6	F: 5'-AACGAACACATCCACCGGCTCTC-3'	PROK2	F: 5'-ACAAGGACTCCCAATGTGGT-3'
	R: 5'-GTGGCTATACTCAGCGTAGCGCAG-3'		R: 5'-ATGGAACTTTACGAGTCAGTGG-3'
CP	F: 5'-AGAGCAGAAGTGTGCCTCCT-3'	SELE	F: 5'-GCAACTTCACCTGTGAGGAA-3'
	R: 5'-TAGTGGGATCCACAGCAGAA-3'		R: 5'-GCACTGGAAAGCTTCACAAA-3'
COCH	F: 5'-GCCTATCCCTGAAGAACTGG-3'	SAA2	F: 5'-AGTGATCAGCAATGCCAGAG-3'
	R: 5'-TTGGGCATGTGGTAAGAGAA-3'		R: 5'-AGCAGGTCGGAAGTGATTG-3'
ELOVL7	F: 5'-TTCCATCATACCATCATGCC-3'	TTR	F: 5'-TGAGCATGCAGAGGTGGTAT-3'
	R: 5'-CCCAATGCAGAAAGTCCATA-3'		R: 5'-GGTCCACTGGAGGAGAAGTC-3'
EIF4E	F: 5'-GCTACTAAGAGCGGCTCCAC-3'	SORCS3	F: 5'-CAGAGAACAACCTTGGCTCA-3'
	R: 5'-CTTTGGTTCAGCTCCCAAAT-3'		R: 5'-TGCACTGATGTTGACCTCCT-3'
FN1	F: 5'-GCAGAGGCATAAGGTTCGGGAAG-3'	WIF1	F: 5'-GTGTGAAATCAGCAAATGCC-3'
	R: 5'-GGGAAACTGTGTAGGGGTCAAAGC-3'		R: 5'-CTCCCTGGTAACCTTTGGAA-3'
GPR146	F: 5'-TACGAAAGAATGGCAACAGC-3'		
	R: 5'-TTCTCAGAACCCTGTGGTGA-3'		

TABLE 3.

Gene name	Unigene	TM-Tissue (SV±SD)	TM-Cells (SV±SD)	[9]	[8]	[11]	[12]
Beta actin	ACTB	29338.7±4900.8	45504.0±13031.0	*	*	*	**
Calreticulin	MNT	27317.0±7448.7	32472.2±27730.8	*			*
Matrix Gla protein	MGP	26948.0±6100.0	30903.3±13352.6	**	**	*	*
Tumor protein, translationally controlled 1	TPT1	25270.3±5290.6	33857.7±7219.6	**		**	*
Heterogeneous nuclear ribonucleoprotein A1	HNRPA1	24886.7±4085.1	30312.0±11590.7	*			*
Chitinase 3-like 1	CHI3L1	24598.3±4220.7	39115.3±13522.0	*	**		**
Heterogeneous nuclear ribonucleoprotein H1	HNRPH1	24576.3±3208.4	20595.0±12332.5	*			*
Calponin 3, acidic	CNN3	22844.0±3750.4	21742.0±16406.3	*			*
Metastasis-associated lung adenocarcinoma transcript 1	MALAT1	22386.0±1582.3	21798.3±15656.1				
Amyloid beta (A4) precursor protein	APP	22323.0±7007.3	21240.7±15793.5			**	*
H3 histone, family 3A	H3F3A	21357.3±2846.2	26101.3±11870.1		*	*	*
Nuclear ubiquitous casein kinase/ cyclin-dependent kinase substrate	NUCKS	21013.0±4169.4	20936.3±13559.1	*			
Tissue inhibitor of metalloproteinase 2	TIMP2	20966.3±2314.1	28300.0±8642.6	*			*
Heat shock 90 kDa protein 1, alpha	HSPCA	20751.3±6126.9	25471.3±9332.5	*		*	*
Heterogeneous nuclear ribonucleoprotein K	HNRPK	20493.7±3298.0	21150.7±8755.2	*			*
ATP synthase, H+ transporting, mitochondrial F1 complex, epsilon subunit	ATP5E	20445.7±3525.3	28864.0±15308.5	*			
ATPase, H+ transporting, lysosomal 9 kDa, V0 subunit e	ATP6V0E	20388.7±1447.9	19010.2±15830.0	*			*
Mortality factor 4 like 2	MORF4L2	20365.3±6236.3	25724.7±9497.2				
SMT3 suppressor of mif two 3 homolog 2 (yeast)	SUMO2	20276.3±4859.2	24991.3±13212.0	*			*
CD59 antigen p18-20	CD59	20138.7±2108.3	19595.7±6500.0	*		*	*
High-mobility group nucleosomal binding domain 2	HMGN2	19939.7±4243.4	19998.3±9536.1	*			*
Interferon induced transmembrane protein 3 (1-8U)	IFITM3	19864.7±331.9	22892.0±2719.0		*		**
Tyrosine 3-monooxygenase/ tryptophan 5-monooxygenase activation protein	YWHAE	19845.7±2765.7	21488.7±11620.9	*			*
Transmembrane 4 superfamily member 1	TM4SF1	19822.7±1445.5	24529.0±10827.0	*	*	*	*
Calnexin	CANX	19817.0±2297.7	21184.0±10323.6	*		*	*

Summary of 25 genes sharing the highest signal values in both normal native tissue and cultured human trabecular meshwork (HTM) cells. The Unigene site is provided in the public domain by the National Center for Biotechnology Information, Bethesda, MD. The asterisk indicates that transcripts are represented and the double asterisk indicates that the transcripts are highly represented in the libraries from postmortem trabecular meshwork (TM), perfused TM, infant primary TM culture, and from gene expression profile of cultured HTM using the U95Av2 Affymetrix microarrays (12,626 probe sets). The term SV indicates signal value.

primer and Superscript II reverse transcriptase (Invitrogen, Carlsbad, CA) according to the manufacturer's instructions. Real-time PCR reactions were performed in a 20 µl mixture containing 1 µl of the cDNA preparation, 1X iQ SYBR Green Supermix (Biorad, Hercules, CA) and 500 nm of each primer, in the Bio-Rad iCycler iQ system (BioRad, Hercules, CA) using the following PCR parameters: 95 °C for 5 min followed by 50 cycles of 95 °C for 15 s, 60 °C for 15 s, and 72 °C for 15 s. The fluorescence threshold value (Ct) was determined using the iCycle iQ system software. Expression levels were represented as the inverse of the normalized mean Ct value (InvCt). Eukaryotic translation initiation factor 4E (EIF4E) served as an internal standard of mRNA expression. The absence of nonspecific products was confirmed by both the analysis of the melt curves and electrophoresis in 3% Super AcrylAgarose gels. The sequences of the primers used for the amplifications are indicated in Table 2.

RESULTS

Gene expression profile of trabecular meshwork: To generate a genome-wide comprehensive gene expression profile of the TM, total RNA (20 ng) from three different cultured TM cell lines and the TM from three pairs of control donors was amplified, independently hybridized to Affymetrix Human Genome U133 Plus 2.0 GeneChip microarrays, and analyzed as detailed in the Methods. The full list of gene expression data, including those for the two additional samples from POAG donors, is published online in the Gene Expression Omnibus (GEO) database (accession number: GSE4316). Figure 1 summarizes the number of transcripts expressed in cultured cells and TM tissue. Table 3 summarizes the 25 genes sharing the highest signal values in both cultured and native TM cells compared with the previously published cDNA libraries from TM tissue [8,9], a cDNA library from infant TM primary culture [11], and the gene expression profile of nonamplified HTM

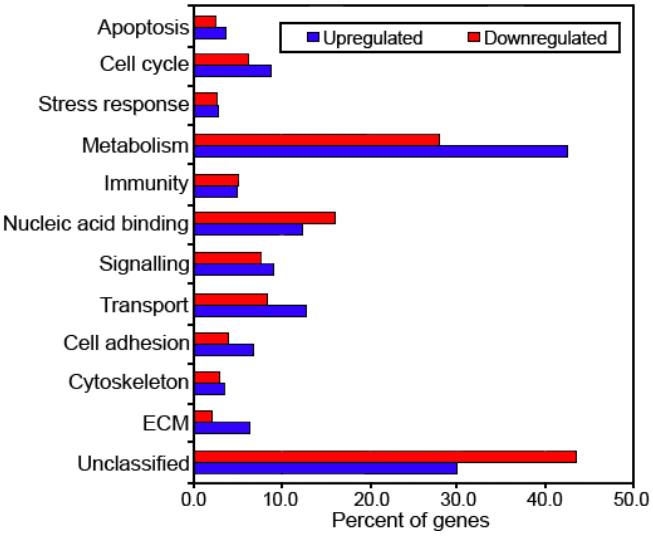

Figure 2. Functional distribution of the genes differentially expressed in cultured human trabecular meshwork (HTM) cells compared to HTM tissue.

TABLE 4.

Gene name	Unigene	Fold change	p value
Cartilage linking protein 1	HAPLN1	147.8	0.0036
Microfibril-associated glycoprotein-2	MFAP5	38.1	0.0029
Fibronectin 1	FN1	37.9	0.0009
Collagen, type XIV, alpha 1	COL14A1	35.7	0.0029
Collagen, type XI, alpha 1	COL11A1	28.5	0.0066
Vitronectin	VTN	26.1	0.0011
Periostin, osteoblast specific factor	POSTN	25.8	0.0478
Spondin 2, extracellular matrix protein	SPON2	21.7	0.0117
Collagen, type VI, alpha 1	COL6A1	20.3	0.0092
Lysyl oxidase	LOX	19.7	0.0068
Collagen, type VI, alpha 2	COL6A2	17.5	0.0154
Collagen, type V, alpha 2	COL5A2	17.5	0.0052
Chordin-like 2	CHRDL2	17.2	0.0353
Lysyl oxidase-like 2	LOXL2	13.7	0.0011
Follistatin	FST	12.6	0.0004
Collagen, type III, alpha 1	COL3A1	12.4	0.0007
Laminin, gamma 1	LAMC1	8.9	0.001
Fibronectin leucine rich transmembrane protein 2	FLRT2	7.6	0.0161
Collagen, type I, alpha 1	COL1A1	7.2	0.0003
Collagen, type XII, alpha 1	COL12A1	6.5	0.0074
Thrombospondin 3	THBS3	6	0.0001
Extracellular matrix protein 1	ECM1	5.8	0.0005
Collagen triple helix repeat containing 1	CTHRC1	5.2	0.0074

ECM-related genes upregulated (>5 fold) in cultured human trabecular meshwork (HTM) cells.

primary cultures using the U95Av2 Affymetrix microarrays (12,626 probe sets) [12]. To simplify the data, we have excluded from the list the generally highly expressed ribosomal proteins and elongation factors. Matrix Gla Protein (MGP), chitinase 3-like 1 (CHI3L1), and the ubiquitously expressed tumor protein translationally controlled 1 (TPT1) were found to be present at high levels in at least three out of the five studies.

Genes differentially expressed in trabecular meshwork tissue and human trabecular meshwork cultured cells: The gene expression profile of cultured TM cells was compared to that of control TM tissue. The full lists of genes differentially expressed at least two fold with a p value lower than 0.05 is included in Appendix 1. In summary, 657 genes were found to be upregulated and 2,646 genes were downregulated in cultured TM cells compared to native TM tissue. Figure 2 represents the functional distribution of the differentially expressed genes. It is worth noting that most of the genes showing the highest upregulated differential fold expression are involved in the maintenance of the extracellular matrix (ECM), including matricellular proteins (microfibril-associated glycoprotein-2 and spondin 2), leptins (fibronectin-1 and vitronectin), several types of collagens, as well as proteins involved in the synthesis of the ECM (cartilage linking protein 1 and lysyl oxidase; Table 4). Among the genes downregulated in cultured TM cells, the highest proportion (43%) corresponded to unknown genes or genes still not associated with cellular function. Table 5 lists genes down regulated in cultured TM cells whose functions may be important or have already been associated with the maintenance of TM tissue functionality, such as cochlin, aquaporin, and adenosine A3 receptor. Of particular interest is the downregulation of the genes highly expressed in native TM tissue: myocilin, angiopoietin-like factor, and apolipoprotein D (Appendix 1; Downregulared genes).

Differential gene expression profile analysis between control and primary open angle glaucoma donors: The gene expression profile of the TM from the two analyzed POAG samples revealed relatively small changes compared to that of control donors. A total of 156 genes showed a significant average fold-change value greater than 2 in POAG tissue; 72 genes were upregulated (Table 6), and 84 genes were downregulated (Table 7). Among all these genes, selectin-E (ELAM-I) demonstrated the highest differential transcriptional levels (31 fold induction), as well as restricted expression to POAG samples. mRNA for this gene was not detected in either control TM tissue or cultured TM cells. Together with selectin-E, the TM from POAG tissue showed an upregulation of several genes coding for proteins involved in inflammation and acute-phase response, such as chemokine (C-X-C motif) ligand 6, chemokine (C-C motif) ligand 5, immune-associated nucleotide, interleukin 1 receptor type II, transthyretin, haptoglobin, and myelin basic protein. Other genes upregulated

TABLE 5.

Gene name	Unigene	Fold change	p value
Serum amyloid A2	SAA1	194.7	0.000622
Endothelin 3	EDN3	169.3	0.0000759
Tachykinin, precursor 1	TAC1	156.5	0.00108
Ceruloplasmin	CP	146	0.0000125
Integrin, alpha 9	ITGA9	127.2	0.000216
Cochlin	COCH	125	0.000803
Aquaporin 1	AQP1	107.5	0.000468
WNT inhibitory factor 1	WIF1	89.05	0.0151
Adrenergic, beta-1-, receptor	ADRB1	83.21	0.00119
Purinergic receptor P2Y, G-protein coupled, 12	P2RY12	73.23	0.0048
Endothelin receptor type B	EDNRB	68.77	0.000207
Latrophilin 3	LPHN3	66.7	0.00304
Regulator of G-protein signaling 1	RGS1	61.49	0.00191
Adrenergic, alpha-2A-, receptor	ADRA2A	60.12	0.00372
Angiopoietin-like factor	CDT6	43.95	0.000396
Frizzled homolog 10	FZD10	38.36	0.00155
Matrix metalloproteinase 3	MMP3	28.8	0.0136
Apolipoprotein D	APOD	25.75	0.00000206
Matrix metalloproteinase 10	MMP10	23.07	0.0094
Carbonic anhydrase XIV	CA14	22.85	0.0107
Adenosine A3 receptor	ADORA3	18.72	0.0044
Adrenergic, beta-2-, receptor, surface	ADRB2	16.7	0.00589
Glutathione S-transferase theta 2	GSTT2	13.44	0.0109
Haptoglobin	HP	10.68	0.0145
Myocilin	MYOC	7.228	0.0000878

List of the selected genes downregulated in cultured human trabecular meshwork (HTM) cells compared to trabecular meshwork (TM) tissue.

TABLE 6.

Gene name	Unigene	Fold change	p value	Control TM
selectin E (endothelial adhesion molecule 1)	SELE	31.08	0.0258	A-A-A
testes development-related NYD-SP21	NYD-SP21	12.67	0.00513	A-A-A
ELOVL family member 7, elongation of long chain fatty acid	ELOVL7	6.864	0.00908	A-P-A
prokineticin 2	PROK2	6.778	0.00682	A-A-A
BCL2-related protein A1	BCL2A1	6.431	0.0244	P-P-A
SRY (sex determining region Y)-box 17	SOX17	4.236	0.0446	P-A-P
neural precursor cell expressed, developmentally down-regulated 9	NEDD9	4.184	0.00521	P-P-P
LIM domain only 7	LMO7	3.706	0.0201	P-P-P
protocadherin 17	LOC144997	3.422	0.0481	P-P-A
membrane protein, palmitoylated 3 (MAGUK p55 subfamily member 3)	MPP3	3.237	0.0173	M-M-P
solute carrier family 16 (monocarboxylic acid transporters), member 6	SLC16A6	3.016	0.0378	P-P-P
transthyretin (prealbumin, amyloidosis type I)	TTR	2.945	0.00554	A-P-P
Microfibril-associated glycoprotein-2	MAGP2	2.849	0.00292	A-A-A
hypoxia-inducible protein 2	HIG2	2.838	0.00298	P-P-P
ecotropic viral integration site 1	EVI1	2.809	0.0195	P-P-A
G protein-coupled receptor 146	GPR146	2.78	0.0376	P-P-P
oxysterol binding protein-like 6	OSBPL6	2.777	0.00563	P-P-A
haptoglobin	HP	2.76	0.0145	P-P-P
chemokine (C-X-C motif) ligand 6 (granulocyte chemotactic protein 2)	CXCL6	2.713	0.000373	P-M-P
immune associated nucleotide	hIAN7	2.695	0.000109	P-P-P
zinc finger protein 36, C3H type, homolog (mouse)	ZFP36	2.686	0.0368	P-P-P
synaptotagmin IV	SYT4	2.635	0.0101	P-A-P
lunatic fringe homolog (Drosophila)	LFNG	2.621	0.0073	P-A-A
regulator of G-protein signalling 1	RGS1	2.537	0.00191	P-P-P
neuropeptide Y receptor Y2	NPY2R	2.535	0.0176	A-A-P
v-fos FBJ murine osteosarcoma viral oncogene homolog	FOS	2.521	0.0134	P-P-A
transient receptor potential cation channel, subfamily M, member 1	TRPM1	2.468	0.0315	P-P-P
matrix metalloproteinase 1 (interstitial collagenase)	MMP1	2.463	0.0393	P-A-A
neuropilin (NRP) and tolloid (TLL)-like 2	NETO2	2.416	0.0362	P-P-P
Epstein-Barr virus induced gene 2	EBI2	2.41	0.00647	P-P-P
adenosine A3 receptor	ADORA3	2.393	0.0044	P-P-P
interleukin 1 receptor, type II	IL1R2	2.388	0.0233	P-A-A
chemokine (C-C motif) ligand 15	CCL15	2.366	0.0107	P-P-P
tripartite motif-containing 16	TRIM16	2.352	0.0215	P-M-P
platelet activating receptor homolog	H963	2.324	0.000568	P-P-A
ribonuclease, RNase A family, k6	RNASE6	2.253	0.00015	P-M-A
membrane-spanning 4-domains, subfamily A, member 7	MS4A7	2.227	0.00326	P-P-P
protein tyrosine phosphatase, non-receptor type 4 (megakaryocyte)	PTPN4	2.175	0.0222	P-A-P
Bruton agammaglobulinemia tyrosine kinase	BTK	2.159	0.000247	P-A-A
myelin basic protein	MBP	2.149	0.0183	P-P-A
chloride intracellular channel 2	CLIC2	2.148	0.0377	P-P-P
Fc fragment of IgG, high affinity Ia, receptor for (CD64)	FCGR1A	2.142	0.00185	P-P-P
F-box only protein 4	FBXO4	2.116	0.0061	P-P-P
cadherin 19, type 2	CDH19	2.055	0.00322	P-P-P
carbohydrate (chondroitin 4) sulfotransferase 12	CHST12	2.05	0.0221	P-M-P
CD1D antigen, d polypeptide	CD1D	2.044	0.00277	P-P-P
delta sleep inducing peptide, immunoreactor	DSIPI	2.038	0.00392	P-P-P
insulin-like growth factor 2 (somatomedin A)	IGF2	2.018	0.0051	P-P-P

List of the known genes significantly upregulated in POAG trabecular meshwork (TM) tissue. Genes were present in all of the POAG samples. The presence of (P), marginal (M), or absence of (A) a signal in each of the three control samples is indicated in the Control TM column.

TABLE 7.

Gene name	Unigene	Fold change	p value	POAG TM
VPS10 domain receptor protein SORCS 3	SORCS3	9.021	0.0026	A
mitogen-activated protein kinase 6	MAP2K6	5.794	0.0108	P
cadherin 10, type 2 (T2-cadherin)	CDH10	5.041	0.00537	P,A
TPTE and PTEN homologous inositol lipid phosphatase pseudogene	TPTEps1	4.992	0.000971	A
calbindin 1, 28 kDa	CALB1	4.907	0.00917	P,M
leucine-rich, glioma inactivated 1	LGI1	3.976	0.00129	P
matrix metalloproteinase 10 (stromelysin 2)	MMP10	3.97	0.0094	P
testis expressed sequence 15	TEX15	3.821	0.0317	A
WNT inhibitory factor 1	WIF1	3.774	0.0151	P
carboxylesterase 1 (monocyte/macrophage serine esterase 1)	CES1	3.352	0.0417	P,A
growth arrest-specific 7	GAS7	3.186	0.0365	P,A
protein kinase, lysine deficient 4	PRKWNK4	3.117	0.0145	P
cytochrome P450, family 39, subfamily A, polypeptide 1	CYP39A1	3.1	0.000473	P
glycoprotein hormone alpha 2	GPHA2	3.012	0.000588	P
ATP-binding cassette, sub-family A (ABC1), member 9	ABCA9	2.822	0.00679	A
purinergic receptor P2Y, G-protein coupled, 12	P2RY12	2.684	0.0048	P,A
nebulin	NEB	2.627	0.00939	P
cortactin binding protein 2	CORTBP2	2.575	0.0111	P
proprotein convertase subtilisin/kexin type 1 inhibitor	PCSK1N	2.575	0.0259	P
paraoxonase 3	PON3	2.523	0.006	A
solute carrier family 10, member 4	SLC10A4	2.496	0.000439	P
cancer susceptibility candidate 1	CASC1	2.436	0.0188	P
solute carrier family 35, member D1	SLC35D1	2.296	0.00196	P
ceruloplasmin	CP	2.282	0.00137	P
tripartite motif protein TRIM9 isoform alpha (TRIM9)	TRIM9	2.235	0.0246	P
protocadherin beta 6	PCDHB6	2.223	1.49E-05	P
cadherin-like 24	CDH24	2.221	0.00234	A
low density lipoprotein-related protein 1B (deleted in tumors)	LRP1B	2.221	0.0183	P
solute carrier family 6 (neurotransmitter transporter, GABA), member 1	SLC6A1	2.218	0.00295	P
frizzled homolog 10 (Drosophila)	FZD10	2.18	0.00155	P
H19, imprinted maternally expressed untranslated mRNA	H19	2.179	0.00277	P
adrenergic, beta-2-, receptor, surface	ADRB2	2.157	0.00589	P
serine protease EOS	EOS	2.146	0.00748	P,A
X transporter protein 3	SLC6A20	2.115	0.00243	P
delta-notch-like EGF repeat-containing transmembrane	DNER	2.11	0.011	P,M
protein phosphatase 1, regulatory (inhibitor) subunit 1B	PPP1R1B	2.089	0.0198	P
B-cell CLL/lymphoma 6, member B (zinc finger protein)	BCL6B	2.078	0.0495	P,M
iduronidase, alpha-L-	IDUA	2.052	0.00162	A
GATA binding protein 6	GATA6	2.04	0.0433	P
EGF-like-domain, multiple 6	EGFL6	2.035	0.00526	P
SMA3	LOC153561	2.023	0.0141	P
EH-domain containing 3	EHD3	2.015	0.0307	P,A
sortilin-related receptor, L(DLR class) A repeats-containing	SORL1	2.009	0.000666	P
acyl-Coenzyme A dehydrogenase, long chain	ACADL	2.005	0.000153	A

List of the known genes significantly downregulated in POAG trabecular meshwork (TM) tissue. Genes were present in all the control samples. The presence of (P), marginal (M), or absence of (A) a signal in each of the two POAG samples is indicated in the POAG TM column.

in POAG samples included ELOVL7 and oxisterol binding protein-like 6, both genes involved in lipid metabolism; several genes related to G-protein signaling regulation, like prokineticin 2, G protein-coupled receptor 146, regulator of G-protein signaling 1, neuropeptide Y receptor Y2, and adenosine A3 receptor; as well as genes involved in ionic transport, such as transient receptor potential cation channel and chloride intracellular channel 2.

Genes downregulated in POAG donors included two members of the vacuolar protein sortin-10 domain receptor family, SORCS3 and SORL1; both the WNT-inhibitory factor 1 and the receptor frizzled homolog 10; several members of the solute carrier family, the mitogen-activated protein kinase 6, ceruloplasmin, as well as paraoxonase 3, an inhibitor of LDL oxidation.

Confirmation of gene microarray analysis by real-time PCR: To further confirm the results of the microarray analysis, we chose a subset of genes differentially expressed among cultured TM cells, control TM tissue, and TM tissue from POAG donors for validation by real-time PCR analysis in nonamplified RNA. With the exception of some small differences at the level of statistical significance, these 24 genes were shown to have consistent trends of change by both microarray analysis and real-time quantitative PCR (Figure 3).

Glaucoma candidate genes: Among all the genes expressed in TM tissue, 929 genes were identified in the 11 loci described to be linked to different forms of glaucoma (Table 8). The complete list of genes is available upon request. To narrow the search for glaucoma candidate genes, we also evaluated the chromosomal location of the genes significantly downregulated in cultured HTM cells compared to TM tissue (Table 9), as well as the genes showing significant differential expression between control and POAG TM tissue (Table 10).

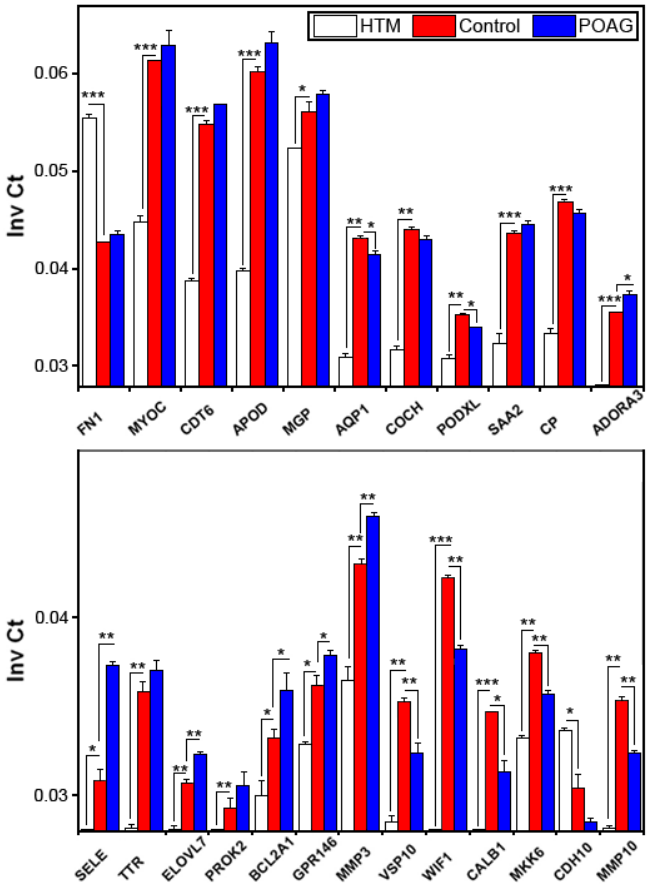

Figure 3. Real-time confirmation of selected genes with differential expression among cultured human trabecular meshwork (HTM) cells, HTM tissue, and POAG trabecular meshwork (TM) tissue. Expression levels are represented as the inverse normalized mean Ct value±SD. Inv Ct values below 0.028 (Ct >35 cycles) were confirmed as primer-dimer products and are not included in the graphic. EIF4-α, which showed no variance in the expression levels between cultured HTM cells and TM tissue, was used for normalization. The single asterisk indicates a $p<0.05$, the double asterisk indicates a $p<0.001$, and the triple asterisk indicates a $p<0.0001$ (t-test, n=3).

TABLE 8.

Gene	TM tissue: Control and POAG	TM tissue: Control specific	TM tissue: POAG specific	Downregulated in Cells	Upregulated in POAG	Downregulated in POAG
GLC1A (1q23-24)	121	3	13	28	2	0
GLC1B (2cen-q13)	66	2	15	9	1	0
GLC1C (3q21-24)	111	4	13	31	1	2
GLC1D (8q23)	24	0	2	3	0	0
GLC1E (10p14)	36	1	3	3	0	0
GLC1F (7q35-36)	79	6	12	17	1	1
GLC1G (5q22)	46	1	2	11	0	0
15q11-13	56	1	5	15	2	0
GLC3A (2p22.2)	22	0	1	6	0	0
GLC3B (1p36.2-36.1)	195	4	25	31	0	0
GLC3C (14q24.3)	56	1	3	13	1	0
Total genes	812	23	94	167	8	3

Summary of glaucoma candidate genes. The trabecular meshwork (TM) tissue list is available upon request.

Table 9. List of the genes downregulated in cultured human trabecular meshwork (HTM) mapping in glaucoma loci.

Locus	Gene	Unigene	Unigene ID cluster
GLC1A	Activating transcription factor 6	ATF6	Hs.433046
	ATPase, Na+/K+ transporting, alpha 2 (+) polypeptide	ATP1A2	Hs.34114
	AV712694 DCA Homo sapiens cDNA clone DCAAJG07 5', mRNA sequence.	KIFAP3	
	CD1D antigen, d polypeptide	CD1D	Hs.1799
	CDNA FLJ13332 fis, clone OVARC1001813		Hs.225093
	Coagulation factor V (proaccelerin, labile factor)	F5	Hs.30054
	DnaJ (Hsp40) homolog, subfamily C, member 6	DNAJC6	Hs.129587
	Expressed in hematopoietic cells, heart, liver	HHL	Hs.495257
	Fc fragment of IgE, high affinity I, receptor for; gamma polypeptide	FCER1G	Hs.433300
	Fc fragment of IgG, low affinity IIa, receptor for (CD32)	FCGR2A	Hs.352642
	Fc fragment of IgG, low affinity IIb, receptor for (CD32)	FCGR2B	Hs.126384
	FLJ45235 protein	FLJ45235	Hs.130054
	Homo sapiens Fc fragment of IgE, high affinity I, receptor for; gamma polypeptide, mRNA (cDNA clone MGC:22620 IMAGE:4704425), complete cds.	FCER1G	
	Hypothetical protein FLJ10287	FLJ10287	Hs.40337
	Hypothetical protein FLJ20442	FLJ20442	Hs.425801
	Hypothetical protein LOC57821	LOC57821	Hs.130746
	Hypothetical protein MGC21854	MGC21854	Hs.233125
	Lamina-associated polypeptide 1B	LAP1B	Hs.234265
	Mitochondrial ribosomal protein S14	MRPS14	Hs.247324
	Myocilin, trabecular meshwork inducible glucocorticoid response	MYOC	Hs.78454
	Selectin L (lymphocyte adhesion molecule 1)	SELL	Hs.82848
	SPT3-associated factor 42	STAF42	Hs.435967
	Tenascin N	TNN	Hs.156369
	Torsin family 3, member A	TOR3A	Hs.26267
	Vang-like 2 (van gogh, Drosophila)	VANGL2	Hs.137507
	Vesicle-associated membrane protein 4	VAMP4	Hs.6651
	V-ski sarcoma viral oncogene homolog (avian)	SKI	Hs.2969
	Wa37f07.x1 NCI_CGAP_Kid11 Homo sapiens cDNA clone IMAGE:2300293 3', mRNA sequence.	DNM3	
GLC1B	NCK adaptor protein 2	NCK2	Hs.101695
	Pleckstrin homology, Sec7 and coiled-coil domains, binding protein	PSCDBP	Hs.270
	POU domain, class 3, transcription factor 3	POU3F3	Hs.248158
	RAN binding protein 2	RANBP2	Hs.199179
	RAN binding protein 2-like 1	GCC2	Hs.434959
	REV1-like (yeast)	REV1L	Hs.443077
	Ribosomal protein L31	TBC1D8	Hs.375921
	Transcribed sequence with strong similarity to protein prf:2115329A (H.sapiens) 2115329A nucleoprotein Nup358 [Homo sapiens]	DKFZp686P0288	Hs.516168
	Unc-50 homolog (C. elegans)	UNC50	Hs.13370
GLC1C	ATPase, Ca++ transporting, type 2C, member 1	ATP2C1	Hs.106778
	B aggressive lymphoma gene	BAL	Hs.131315
	CD86 antigen (CD28 antigen ligand 2, B7-2 antigen)	CD86	Hs.27954
	Ceruloplasmin (ferroxidase)	CP	Hs.282557
	disrupted in renal carcinoma 2	DIRC2	Hs.11360
	EphB1	EPHB1	Hs.272311
	G protein-coupled receptor 105	GPR105	Hs.2465
	General transcription factor IIE, polypeptide 1, alpha 56 kDa	GTF2E1	Hs.145381
	Hermansky-Pudlak syndrome 3	CP	Hs.282804
	HSPC056 protein	HSPC056	Hs.102708
	Hypothetical protein FLJ10546	FLJ10546	Hs.518278
	Hypothetical protein FLJ10618	FLJ10618	Hs.144130
	Hypothetical protein FLJ23751	FLJ23751	Hs.312930
	Hypothetical protein LOC132241	LOC132241	Hs.437334

Table 9. continued.

Locus	Gene	Unigene	Unigene ID cluster
	Hypothetical protein MGC3040	MGC3040	Hs.280740
	Integrin, beta 5	ITGB5	Hs.149846
	KIAA0779 protein	KIAA0779	Hs.362996
	Kruppel-like factor 15	KLF15	Hs.272215
	Oxysterol binding protein-like 11	OSBPL11	Hs.61260
	Pphospholipid scramblase 1	PLSCR1	Hs.348478
	Protein phosphatase 2 (formerly 2A), regulatory subunit B'', alpha	PPP2R3A	Hs.133234
	Purinergic receptor P2Y, G-protein coupled, 12	P2RY12	Hs.444983
	Rhysin 2	BBAP	Hs.334875
	Ribosomal protein S6 kinase, 90 kDa, polypeptide 1	RPS6KA1	Hs.149957
	Serine/threonine kinase with Dbl- and pleckstrin homology domains	TRAD	Hs.162189
	Solute carrier family 15 (H+/peptide transporter), member 2	SLC15A2	Hs.118747
	Sorting nexin 4	SNX4	Hs.267812
	Transcription factor Dp-2 (E2F dimerization partner 2)	TFDP2	Hs.379018
	Transmembrane protein 22	TMEM22	Hs.101257
	Zinc finger protein 148 (pHZ-52)	ZNF148	Hs.442787
	Zinc finger protein 9 (a cellular retroviral nucleic acid binding protein)	ZNF9	Hs.2110
GLC1D	Angiopoietin 1	ANGPT1	Hs.2463
	Hypothetical protein MGC35555	MGC35555	Hs.209569
	Proenkephalin	PENK	Hs.339831
GLC1E	Adenovirus 5 E1A binding protein	ZMYND11	Hs.145894
	Coiled-coil domain containing 3	CCDC3	Hs.107253
	DNA-damage-inducible transcript 4	DDIT4	Hs.111244
GLC1F	CDNA clone IMAGE:6183232, partial cds		Hs.491104
	CDNA FLJ46106 fis, clone TESTI2026284		Hs.308222
	df18g11.y1 Morton Fetal Cochlea Homo sapiens cDNA clone IMAGE:2483901 5', mRNA sequence.		
	DnaJ (Hsp40) homolog, subfamily B, member 6	DNAJB6	Hs.181195
	Hepatocellular carcinoma-associated antigen 112	HCA112	Hs.12126
	Human immune associated nucleotide 2	hIAN2	Hs.105468
	Immune associated nucleotide	hIAN7	Hs.124675
	Immune associated nucleotide 4 like 1 (mouse)	IAN4L1	Hs.412331
	Immunity associated protein 4	HIMAP4	Hs.30822
	KIAA1718 protein	KIAA1718	Hs.222707
	LR8 protein	LR8	Hs.190161
	Protein tyrosine phosphatase, receptor type, N polypeptide 2	PTPRN2	Hs.74624
	SWI/SNF related, matrix associated, actin dependent regulator of chromatin, subfamily d, member 3	SMARCD3	Hs.444445
	Th95b11.x1 Soares_NSF_F8_9W_OT_PA_P_S1 Homo sapiens cDNA clone IMAGE:2126397 3', mRNA sequence.	IAN4L1	
	Tt37g06.x1 NCI_CGAP_GC6 Homo sapiens cDNA clone IMAGE:2243002 3' similar to contains MER13.t1 MER13 repetitive element, mRNA sequence.	hIAN6	
	Wp61g11.x1 NCI_CGAP_Brn25 Homo sapiens cDNA clone IMAGE:2466308 3', mRNA sequence.	LOC154761	
	Zinc finger protein 212	ZNF212	Hs.108139
GLC1G	601661186R1 NIH_MGC_72 Homo sapiens cDNA clone IMAGE:3916173 3', mRNA sequence.	MCC	
	APG12 autophagy 12-like (S. cerevisiae)	APG12L	Hs.264482
	COMM domain containing 10	COMMD10	Hs.151458
	Cysteine dioxygenase, type I	CDO1	Hs.442378
	Decapping enzyme hDcp2	DCP2	Hs.442039
	Glutathione peroxidase 3 (plasma)	GPX3	Hs.386793
	Praja 2, RING-H2 motif containing	PJA2	Hs.224262
	Sema domain, transmembrane domain (TM), and	SEMA6A	Hs.443012

Table 9. continued.

Locus	Gene	Unigene	Unigene ID cluster
	Cytoplasmic domain, (semaphorin) 6A		
	TIGA1	TIGA1	Hs.12082
	Tripartite motif-containing 36	TRIM36	Hs.429642
	Ubiquitin-conjugating enzyme E2B (RAD6 homolog)	UBE2B	Hs.385986
GLC3A	Adenylate cyclase 3	ADCY3	Hs.188402
	Baculoviral IAP repeat-containing 6 (apollon)	BIRC6	Hs.360026
	Chromosome 2 open reading frame 8	C2orf8	Hs.368545
	Human Tis11d gene, complete cds.	ZFP36L2	
	Hypothetical protein MGC33926	MGC33926	Hs.40808
	Solute carrier family 8 (sodium/calcium exchanger), member 1	SLC8A1	Hs.144465
GLC3B	Angiopoietin-like factor	CDT6	Hs.146559
	Calmodulin binding transcription activator 1	CAMTA1	Hs.253254
	Chloride channel Kb	CLCNKA	Hs.352243
	Collagen, type XVI, alpha 1	COL16A1	Hs.26208
	Complement component 1, q subcomponent, alpha polypeptide	C1QA	Hs.9641
	Complement component 1, q subcomponent, beta polypeptide	C1QB	Hs.8986
	DnaJ (Hsp40) homolog, subfamily C, member 6	DNAJC6	Hs.129587
	Gardner-Rasheed feline sarcoma viral (v-fgr) oncogene homolog	FGR	Hs.1422
	Hc93h01.x1 Soares_NFL_T_GBC_S1 Homo sapiens cDNA clone IMAGE:2907601 3' similar to contains element MER30 repetitive element, mRNA sequence.	IL28RA	
	Heterogeneous nuclear ribonucleoprotein R	HNRPR	Hs.15265
	Homo sapiens cDNA clone MGC:1167 IMAGE:3536204, complete cds.	ATPIF1	
	Hypothetical protein BC007899	LOC148898	Hs.61884
	Hypothetical protein FLJ10287	FLJ10287	Hs.40337
	Hypothetical protein MGC34648	MGC34648	Hs.96607
	Kinesin family member 1B	KIF1B	Hs.444757
	LOC388610 (LOC388610), mRNA		Hs.355747
	Mitochondrial ribosomal protein L20	MRPL20	Hs.182698
	MRNA; cDNA DKFZp667N1113 (from clone DKFZp667N1113)	RSC1A1	Hs.24183
	Period homolog 3 (Drosophila)	PER3	Hs.418036
	Phosphatidic acid phosphatase type 2B	PPAP2B	Hs.525620
	Phospholipase A2, group IIA (platelets, synovial fluid)	PLA2G2A	Hs.76422
	Phospholipase A2, group V	PLA2G5	Hs.319438
	Protein tyrosine phosphatase type IVA, member 2	PTP4A2	Hs.82911
	Qe51c05.x1 Soares_fetal_lung_NbHL19W Homo sapiens cDNA clone IMAGE:1742504 3' similar to SW:C1QC_HUMAN P02747 COMPLEMENT C1Q SUBCOMPONENT, C CHAIN PRECURSOR; mRNA sequence.	C1QG	
	Retinoid binding protein 7	RBP7	Hs.422688
	Similar to RIKEN cDNA F730108M23 gene (LOC400734), mRNA	GPR157	Hs.31181
	SMART/HDAC1 associated repressor protein	SHARP	Hs.184245
	Solute carrier family 2 (facilitated glucose/fructose transporter), member 5	SLC2A5	Hs.33084
	Synonym: TDP-43; TAR DNA-binding protein-43; go_component: nucleus [goid 0005634; evidence TAS; pmid 7745706]; go_function: microtubule binding [goid 0008017; evidence TAS; pmid 8599929]; go_function: transcription factor activity [goid 0003700; evidence TAS; pmid 8599929]; go_function: RNA binding [goid 0003723] [evidence IEA]; go_process: mitosis [goid 0007067] [evidence TAS; pmid 8599929]; go_process: transcription from Pol II promoter [goid 0006366] [evidence TAS; pmid 7745706]; go_process: mRNA splicing [goid 0006371; evidence IEA]; go_process: regulation of transcription,	TARDBP	

Table 9. continued.

Locus	Gene	Unigene	Unigene ID cluster
	DNA-dependent [goid 0006355; evidence IEA]; go_process: nuclear mRNA splicing, via spliceosome [goid 0000398; evidence IEA]; Homo sapiens TAR DNA binding protein (TARDBP), mRNA.		
	Tumor necrosis factor receptor superfamily, member 1B	TNFRSF1B	Hs.256278
	UBX domain containing 3	UBXD3	Hs.432503
GLC3C	Calmodulin 1 (phosphorylase kinase, delta)	CALM1	Hs.282410
	Chromosome 14 open reading frame 141	LTBP2	Hs.512776
	Chromosome 14 open reading frame 168	C14orf168	Hs.7086
	Chromosome 14 open reading frame 168	C14orf168	Hs.7086
	Chromosome 14 open reading frame 58	C14orf58	Hs.267566
	Ceiodinase, iodothyronine, type II	DIO2	Hs.436020
	Hypothetical protein LOC283578	LOC283578	Hs.212992
	KIAA0759	KIAA0759	Hs.7285
	KIAA1737	KIAA1737	Hs.22452
	Ribonuclease, RNase A family, 2 (liver, eosinophil-derived neurotoxin)	RNASE2	Hs.728
	RNA-binding region (RNP1, RRM) containing 7	RBM25	Hs.197184
	Serine palmitoyltransferase, long chain base subunit 2	SPTLC2	Hs.59403
	Synonym: ACYPE; isoform a is encoded by transcript variant 1; go_function: acylphosphatase activity [goid 0003998; evidence TAS; pmid 7796909]; go_function: hydrolase activity [goid 0016787] [evidence IEA]; go_process: phosphate metabolism [goid 0006796; evidence TAS; pmid 3026468]; Homo sapiens acylphosphatase 1, erythrocyte (common) type (ACYP1), transcript variant 1, mRNA.	ACYP1	
15q11-13	7i87g09.x1 NCI_CGAP_Ov18 Homo sapiens cDNA clone IMAGE:3341728 3', mRNA sequence.	SNRPN	
	AV715153 DCB Homo sapiens cDNA clone DCBBNE07 5', mRNA sequence.	UBR1	
	CDNA FLJ37663 fis, clone BRHIP2011120	LOC283713	Hs.4986
	Hypothetical protein FLJ20313	FLJ20313	Hs.126721
	Hypothetical protein FLJ38426	FLJ38426	Hs.6799
	Likely ortholog of mouse aquarius	AQR	Hs.129952
	Oculocutaneous albinism II (pink-eye dilution homolog, mouse)	OCA2	Hs.82027
	PRO1914 protein	FLJ20582	Hs.5327
	Protein inhibitor of activated STAT, 1	PIAS1	Hs.75251
	Similar to RIKEN cDNA 5730421E18 gene	MGC14798	Hs.149176
	Small nuclear ribonucleoprotein polypeptide N	SNRPN	Hs.48375
	Transient receptor potential cation channel, subfamily M, member 1	TRPM1	Hs.155942
	Transmembrane 6 superfamily member 1	HDGFRP3	Hs.151155
	Ubiquitin protein ligase E3A (human papilloma virus E6-associated protein, Angelman syndrome)	UBE3A	Hs.180686
	Xm51f06.x1 NCI_CGAP_GC6 Homo sapiens cDNA clone IMAGE:2687747 3' similar to contains MER2.b2 MER2 repetitive element; mRNA sequence.	FLJ20582	

DISCUSSION

In this study, we present for the first time, the genome-wide gene expression profile of both cultured HTM cells and native TM tissue, including that of POAG donors, using Affymetrix gene microarrays in conjunction with the novel linear mRNA amplification method, Ribo-SPIA™. This amplification tool, which has been demonstrated to provide an accurate and reliable representation of the transcripts [13,14], allowed us individual hybridizations, thereby preventing potential false positives that might result from pooling RNA from different donors. We performed quantitative real-time PCR analysis of a subset of genes in nonamplified RNA to validate the use of this technique to overcome the limitation of TM size in this type of study.

The comparative gene expression profile analysis of cultured HTM cells showed a high level of similarity to that of native tissue. More than 90% of the genes expressed in the HTM cells in vitro were also present in TM tissue, indicating that cells growing in the culture plates do indeed derive from the TM. To date, no gene strictly specific to the TM has been uncovered. However, the consistent high levels of expression of MGP and CHI3L1 in the TM, together with their restricted pattern of tissue expression, strengthen the potential use of MGP and CHI3L1 as markers for cultured TM cells [12,15].

Despite the high level of similarity, important changes at the gene expression level were found when cultured TM cells were compared to native TM tissue. As recently pointed out by Fautsch et al. [16], TM cells, which rarely replicate in vivo, are “forced” to replicate and grow in bi-dimensional plastic substrates when cultured in vitro. The adaptation to this artificial architecture and environmental cues likely explains the observed increased cellular activity in cultured HTM cells, as well as the upregulation of ECM genes, which are required for the formation of a new biological substrate.

Potentially more relevant to the understanding of outflow pathway physiology are the genes downregulated or even lost in cultured HTM cells. In addition to a three-dimensional structure and the presence of aqueous humor rather than culture rich-media, cells in the outflow pathway are continuously subjected to mechanical forces in situ [17,18]. The absence of such factors in culture conditions could affect the expression of genes essential for outflow pathway functionality in vivo. In addition, since the outflow pathway is composed of different cell types, we cannot rule out the possibility that genes downregulated in cultured conditions are normally expressed in the tissue by cell types that may be underrepresented or absent in primary cultures of HTM cells at passage 3 due to drift in cellular representation. Finally, differences in donor age and post-mortem time could potentially exert some influences in the pattern of gene expression of culture cells.

Although no strictly TM specific genes were identified in this study, many of the genes downregulated in cell culture, such as podocalyxin and angiopoietin-like factor, are known to be involved in specialized functions or present a restricted pattern of tissue distribution indicative of their involvement in specific tissue functions. In contrast, most housekeeping genes did not showed a significant change in the levels of expression in cultured cells. These results suggest some levels of dedifferentiation when subjected to cultured conditions.

Both gene arrays and real-time PCR analysis confirmed the downregulation of three genes highly represented in native TM tissue: *MYOC*, *CDT6*, and *APOD*. Lower expression of *MYOC* in TM cell primary cultures and perfused TM tissue has already been reported [8,11]. Interestingly, expression of *MYOC* is rescued when HTM cells are cultured in DMEM supplemented with aqueous humor instead of standard serum [16], suggesting a critical role of aqueous humor composition for the transcription of *MYOC*. It is more difficult to speculate about the potential causes leading to the downregulation of *CDT6* and *APOD*. *CDT6*, located within the glaucoma locus GLC3B, encodes a secreted angiopoietin-like factor that is also highly expressed in the human corneal stroma where it is

TABLE 10.

Locus	Upregulated in POAG	Downregulated in POAG
GLC1A	Selectin E (endothelial adhesion molecule 1)	None
	CD1D antigen, d polypeptide	None
GLC1B	Interleukin 1 receptor, type II	None
GLC1C	Ecotropic viral integration site 1	Purinergic receptor P2Y, G-protein coupled, 12 ceruloplamin
GLC1D	None	None
GLC1E	None	None
GLC1F	Immune associated nucleotide Homo sapiens cDNA clone IMAGE:2243002 3' similar to contains MER13.t1	cDNA clone IMAGE:6183232, partial cds
15q11-13	Transient receptor potential cation channel, subfamily M, member 1 CDNA FLJ37663 fis, clone BRHIP2011120	None
GLC3A	None	None
GLC3B	None	None
GLC3C	V-fos FBJ murine osteosarcoma viral oncogene homolog	None

List of the genes differentially expressed in POAG trabecular meshwork (TM) mapping glaucoma loci.

thought to influence the deposition of the ECM [19]. The upregulated expression of *CDT6* in cultured HTM cells has been reported after treatment with TGF-β1 and TGF-β2 [20], factors known to be increased in the aqueous humor of pseudoexfoliation glaucoma and POAG donors, respectively. The function of APOD, a carrier protein member of the lipocalins family, and its possible role in the TM remain yet to be determined. Interestingly, the transcription of this gene was significantly induced in the TM of perfused human anterior segments subjected to elevated intraocular pressure [21].

Other genes showing significant downregulated expression in cultured HTM cells and reported to be potentially important in the maintenance of outflow pathway function were aquaporin 1 (*AQP1*) and adenosine A3 receptor (*ADORA3*). AQP1 has been previously localized in the endothelium of the TM and SC in addition to the nonpigmented epithelium of the ciliary processes and the iris epithelium [22,23]. The exact role of AQP1 expression in TM and SC cell function has not yet been demonstrated, although it was hypothesized to influence osmotic permeability of the TM plasma membrane as well as the resting intracellular volume and, thus possibly paracellular permeability [24]. AQP1 deletion in mice has been shown, instead, to decrease IOP by reducing the aqueous humor secretion without affecting outflow resistance [25]. A similar role in modulating IOP by altering both aqueous humor production and outflow facility has been proposed for adenosine receptors [26-28]. ADORA3, in particular, has been shown to increase the rate of aqueous humor secretion by activating the chloride channels in the nonpigmented ciliary epithelial cells [29,30]. This gene has recently been reported to be selectively upregulated in the ciliary epithelium of eyes with pseudoexfoliation syndrome and glaucoma [31]. Interestingly, our analysis also demonstrated increased expression of ADORA3 in the TM of POAG donors. Given its protective role in extraocular tissues against oxidative damage [32,33], as well as its anti-inflammatory effects [34], ADORA3 may be particularly important in pathophysiological mechanisms in the outflow pathway.

Consistent with the absence of dramatic morphological changes, a relatively small number of genes showed significant differential expression between the TM from POAG donors and control samples, which resulted mostly from the high levels of individual variability among the samples. Since stringent criteria were applied in the analysis of the data in order to obtain confident results despite the individual variation and sample size, the small number of observed changes is likely to be an underestimate. It also has to be taken in consideration that, due to the difficulty in obtaining samples from untreated donors, a general limitation of this and other studies including POAG donor tissues results from the fact that glaucoma medication may exert effects on the levels of expression of certain genes. Expression profile analysis did not indicate the upregulation of fibrosis- or calcification-associated genes in the POAG phenotype. Likewise, we did not find increased levels of cochlin mRNA expression associated with POAG, suggesting that the reported accumulation of cochlin in the POAG TM [35,36] might result from decreased protein degradation rather than increased synthesis. The TM from POAG donors showed upregulation of several genes involved in inflammatory and acute-phase responses, including the expression of a previously reported molecular marker of the glaucoma disease phenotype, selectin-E (ELAM-1) [37], which, interestingly, was not found to be expressed either in the control TM tissues or in cultured TM cells. A similar inflammatory phenotype accompanies a large number of age-related diseases such as atherosclerosis, Alzheimer's disease, Parkinson's disease, and rheumatoid arthritis [38].

The expression of inflammatory molecules in aged tissues is believed to result from the production of reactive oxygen species (ROS) and free-radical chain reactions generated from lipid peroxidation [39]. The generation of ROS, which may initiate or contribute to the progression of glaucoma, is likely to occur in the TM, a tissue constantly exposed to an oxidative environment [40,41]. Indeed, decreased antioxidant potential [42,43], increased expression of oxidative stress markers [43], as well as increased oxidative DNA damage [44] and peroxized lipids [45] have been described in the TM of glaucoma patients. Moreover, we have recently reported an accumulation of senescent cells in the glaucomatous outflow pathway [46], which may, in turn, increase the generation of ROS. In addition, the TM from POAG donors demonstrated downregulated expression of the antioxidants, paraoxonase 3 and ceruloplasmin. Interestingly, ceruloplasmin, which also showed downregulated expression in cultured HTM cells and whose mutations are related to several diseases [47-49], is located in the glaucoma locus GLC1C.

In summary, we have generated and compared, for the first time, the genome-wide gene expression profile of cultured HTM cells and TM tissue from both control and POAG donors. Although cultured HTM preserved the TM markers, CHI3L1 and MGP, several differences in gene expression compared to the native TM tissue highlight the importance of developing new conditions for the culture of TM cells capable of preserving the characteristics of TM cells in vivo. Likewise, our profile analysis of POAG TM tissue shows that the TM in POAG does not experience extensive changes in gene expression. Our data suggests that upregulation of genes involved in inflammation and acute phase response might initiate or contribute to the progression of glaucoma. However, the observation of great levels of individual variability indicated that the analysis of a relatively high number of samples will be necessary in the future to obtain a reliable glaucoma signature.

ACKNOWLEDGEMENTS

This work was supported in part by the Research to Prevent Blindness Foundation, and NIH grants EY05722, EY01894, and EY016228.

REFERENCES

1. Sommer A. Intraocular pressure and glaucoma. Am J Ophthalmol 1989; 107:186-8.
2. Bill A, Phillips CI. Uveoscleral drainage of aqueous humour in human eyes. Exp Eye Res 1971; 12:275-81.

3. Quigley HA. Open-angle glaucoma. N Engl J Med 1993; 328:1097-106.
4. Raviola G. Schwalbe line's cells: a new cell type in the trabecular meshwork of Macaca mulatta. Invest Ophthalmol Vis Sci 1982; 22:45-56.
5. Acott TS, Samples JR, Bradley JM, Bacon DR, Bylsma SS, Van Buskirk EM. Trabecular repopulation by anterior trabecular meshwork cells after laser trabeculoplasty. Am J Ophthalmol 1989; 107:1-6.
6. Tripathi RC, Tripathi BJ. Functional anatomy of the chamber angle. In: Jakobiec FA, editor. Ocular anatomy, embryology and teratology. Philadelphia: Harper & Row; 1982. p. 197-248.
7. Lutjen-Drecoll E. Functional morphology of the trabecular meshwork in primate eyes. Prog Retin Eye Res 1999; 18:91-119.
8. Gonzalez P, Epstein DL, Borras T. Characterization of gene expression in human trabecular meshwork using single-pass sequencing of 1060 clones. Invest Ophthalmol Vis Sci 2000; 41:3678-93.
9. Tomarev SI, Wistow G, Raymond V, Dubois S, Malyukova I. Gene expression profile of the human trabecular meshwork: NEIBank sequence tag analysis. Invest Ophthalmol Vis Sci 2003; 44:2588-96.
10. Stamer WD, Seftor RE, Williams SK, Samaha HA, Snyder RW. Isolation and culture of human trabecular meshwork cells by extracellular matrix digestion. Curr Eye Res 1995; 14:611-7.
11. Wirtz MK, Samples JR, Xu H, Severson T, Acott TS. Expression profile and genome location of cDNA clones from an infant human trabecular meshwork cell library. Invest Ophthalmol Vis Sci 2002; 43:3698-704.
12. Liton PB, Liu X, Stamer WD, Challa P, Epstein DL, Gonzalez P. Specific targeting of gene expression to a subset of human trabecular meshwork cells using the chitinase 3-like 1 promoter. Invest Ophthalmol Vis Sci 2005; 46:183-90.
13. Dafforn A, Chen P, Deng G, Herrler M, Iglehart D, Koritala S, Lato S, Pillarisetty S, Purohit R, Wang M, Wang S, Kurn N. Linear mRNA amplification from as little as 5 ng total RNA for global gene expression analysis. Biotechniques 2004; 37:854-7.
14. Singh R, Maganti RJ, Jabba SV, Wang M, Deng G, Heath JD, Kurn N, Wangemann P. Microarray-based comparison of three amplification methods for nanogram amounts of total RNA. Am J Physiol Cell Physiol 2005; 288:C1179-89.
15. Gonzalez P, Caballero M, Liton PB, Stamer WD, Epstein DL. Expression analysis of the matrix GLA protein and VE-cadherin gene promoters in the outflow pathway. Invest Ophthalmol Vis Sci 2004; 45:1389-95.
16. Fautsch MP, Howell KG, Vrabel AM, Charlesworth MC, Muddiman DC, Johnson DH. Primary trabecular meshwork cells incubated in human aqueous humor differ from cells incubated in serum supplements. Invest Ophthalmol Vis Sci 2005; 46:2848-56.
17. Grierson I, Lee WR. Pressure-induced changes in the ultrastructure of the endothelium lining Schlemm's canal. Am J Ophthalmol 1975; 80:863-84.
18. Johnstone MA, Grant WG. Pressure-dependent changes in structures of the aqueous outflow system of human and monkey eyes. Am J Ophthalmol 1973; 75:365-83.
19. Peek R, Kammerer RA, Frank S, Otte-Holler I, Westphal JR. The angiopoietin-like factor cornea-derived transcript 6 is a putative morphogen for human cornea. J Biol Chem 2002; 277:686-93.
20. Zhao X, Ramsey KE, Stephan DA, Russell P. Gene and protein expression changes in human trabecular meshwork cells treated with transforming growth factor-beta. Invest Ophthalmol Vis Sci 2004; 45:4023-34.
21. Vittitow J, Borras T. Genes expressed in the human trabecular meshwork during pressure-induced homeostatic response. J Cell Physiol 2004; 201:126-37.
22. Hamann S, Zeuthen T, La Cour M, Nagelhus EA, Ottersen OP, Agre P, Nielsen S. Aquaporins in complex tissues: distribution of aquaporins 1-5 in human and rat eye. Am J Physiol 1998; 274:C1332-45.
23. Stamer WD, Snyder RW, Smith BL, Agre P, Regan JW. Localization of aquaporin CHIP in the human eye: implications in the pathogenesis of glaucoma and other disorders of ocular fluid balance. Invest Ophthalmol Vis Sci 1994; 35:3867-72.
24. Stamer WD, Peppel K, O'Donnell ME, Roberts BC, Wu F, Epstein DL. Expression of aquaporin-1 in human trabecular meshwork cells: role in resting cell volume. Invest Ophthalmol Vis Sci 2001; 42:1803-11.
25. Zhang D, Vetrivel L, Verkman AS. Aquaporin deletion in mice reduces intraocular pressure and aqueous fluid production. J Gen Physiol 2002; 119:561-9.
26. Karl MO, Fleischhauer JC, Stamer WD, Peterson-Yantorno K, Mitchell CH, Stone RA, Civan MM. Differential P1-purinergic modulation of human Schlemm's canal inner-wall cells. Am J Physiol Cell Physiol 2005; 288:C784-94.
27. Crosson CE. Adenosine receptor activation modulates intraocular pressure in rabbits. J Pharmacol Exp Ther 1995; 273:320-6.
28. Tian B, Gabelt BT, Crosson CE, Kaufman PL. Effects of adenosine agonists on intraocular pressure and aqueous humor dynamics in cynomolgus monkeys. Exp Eye Res 1997; 64:979-89.
29. Do CW, Civan MM. Basis of chloride transport in ciliary epithelium. J Membr Biol 2004; 200:1-13.
30. Civan MM, Macknight AD. The ins and outs of aqueous humour secretion. Exp Eye Res 2004; 78:625-31.
31. Schlotzer-Schrehardt U, Zenkel M, Decking U, Haubs D, Kruse FE, Junemann A, Coca-Prados M, Naumann GO. Selective upregulation of the A3 adenosine receptor in eyes with pseudoexfoliation syndrome and glaucoma. Invest Ophthalmol Vis Sci 2005; 46:2023-34.
32. Hochhauser E, Kaminski O, Shalom H, Leshem D, Shneyvays V, Shainberg A, Vidne BA. Role of adenosine receptor activation in antioxidant enzyme regulation during ischemia-reperfusion in the isolated rat heart. Antioxid Redox Signal 2004; 6:335-44.
33. Maggirwar SB, Dhanraj DN, Somani SM, Ramkumar V. Adenosine acts as an endogenous activator of the cellular antioxidant defense system. Biochem Biophys Res Commun 1994; 201:508-15.
34. Sands WA, Palmer TM. Adenosine receptors and the control of endothelial cell function in inflammatory disease. Immunol Lett 2005; 101:1-11.
35. Bhattacharya SK, Annangudi SP, Salomon RG, Kuchtey RW, Peachey NS, Crabb JW. Cochlin deposits in the trabecular meshwork of the glaucomatous DBA/2J mouse. Exp Eye Res 2005; 80:741-4.
36. Bhattacharya SK, Rockwood EJ, Smith SD, Bonilha VL, Crabb JS, Kuchtey RW, Robertson NG, Peachey NS, Morton CC, Crabb JW. Proteomics reveal Cochlin deposits associated with glaucomatous trabecular meshwork. J Biol Chem 2005; 280:6080-4.
37. Wang N, Chintala SK, Fini ME, Schuman JS. Activation of a tissue-specific stress response in the aqueous outflow pathway of the eye defines the glaucoma disease phenotype. Nat Med 2001; 7:304-9.
38. Sarkar D, Fisher PB. Molecular mechanisms of aging-associated

inflammation. Cancer Lett 2006; 236:13-23.
39. Harman D. The free radical theory of aging. Antioxid Redox Signal 2003; 5:557-61.
40. Spector A, Ma W, Wang RR. The aqueous humor is capable of generating and degrading H2O2. Invest Ophthalmol Vis Sci 1998; 39:1188-97.
41. Garcia-Castineiras S, Velazquez S, Martinez P, Torres N. Aqueous humor hydrogen peroxide analysis with dichlorophenol-indophenol. Exp Eye Res 1992; 55:9-19.
42. Gherghel D, Griffiths HR, Hilton EJ, Cunliffe IA, Hosking SL. Systemic reduction in glutathione levels occurs in patients with primary open-angle glaucoma. Invest Ophthalmol Vis Sci 2005; 46:877-83.
43. Ferreira SM, Lerner SF, Brunzini R, Evelson PA, Llesuy SF. Oxidative stress markers in aqueous humor of glaucoma patients. Am J Ophthalmol 2004; 137:62-9.
44. Sacca SC, Pascotto A, Camicione P, Capris P, Izzotti A. Oxidative DNA damage in the human trabecular meshwork: clinical correlation in patients with primary open-angle glaucoma. Arch Ophthalmol 2005; 123:458-63.
45. Babizhayev MA, Bunin AYa. Lipid peroxidation in open-angle glaucoma. Acta Ophthalmol (Copenh) 1989; 67:371-7.
46. Liton PB, Challa P, Stinnett S, Luna C, Epstein DL, Gonzalez P. Cellular senescence in the glaucomatous outflow pathway. Exp Gerontol 2005; 40:745-8.
47. Horvath R, Freisinger P, Rubio R, Merl T, Bax R, Mayr JA, Shawan, Muller-Hocker J, Pongratz D, Moller LB, Horn N, Jaksch M. Congenital cataract, muscular hypotonia, developmental delay and sensorineural hearing loss associated with a defect in copper metabolism. J Inherit Metab Dis 2005; 28:479-92.
48. Hochstrasser H, Tomiuk J, Walter U, Behnke S, Spiegel J, Kruger R, Becker G, Riess O, Berg D. Functional relevance of ceruloplasmin mutations in Parkinson's disease. FASEB J 2005; 19:1851-3.
49. Panagiotakaki E, Tzetis M, Manolaki N, Loudianos G, Papatheodorou A, Manesis E, Nousia-Arvanitakis S, Syriopoulou V, Kanavakis E. Genotype-phenotype correlations for a wide spectrum of mutations in the Wilson disease gene (ATP7B). Am J Med Genet A 2004; 131:168-73.

The appendix is available in the online version of this article at http://www.molvis.org/molvis/v12/a87/.

The print version of this article was created on 12 Jul 2006. This reflects all typographical corrections and errata to the article through that date. Details of any changes may be found in the online version of the article.